Article

Substituent Effects on Redox Potentials and Optical Gap Energies of Molecule-like Au(SPhX) Nanoparticles

Rui Guo, and Royce W. Murray

J. Am. Chem. Soc., **2005**, 127 (34), 12140-12143• DOI: 10.1021/ja053119m • Publication Date (Web): 06 August 2005

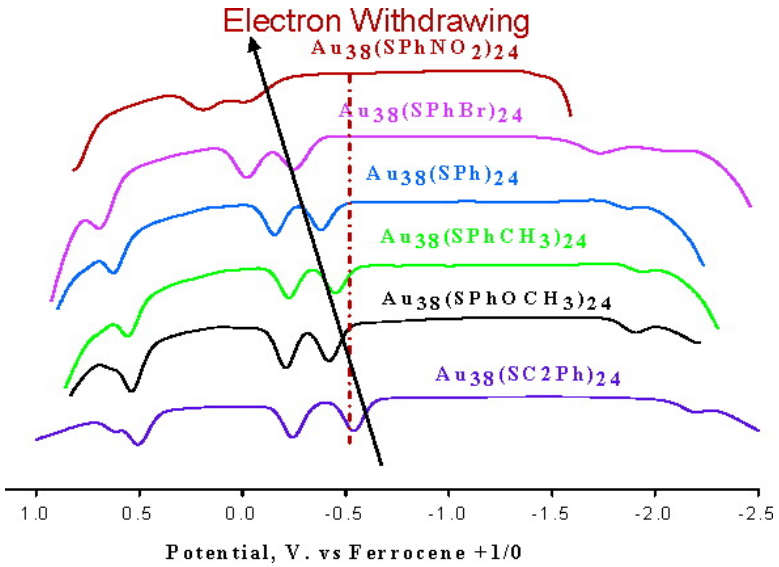

More About This Article

Additional resources and features associated with this article are available within the HTML version:

- Supporting Information
- Links to the 20 articles that cite this article, as of the time of this article download
- Access to high resolution figures
- Links to articles and content related to this article
- Copyright permission to reproduce figures and/or text from this article

View the Full Text HTML

J|A|C|S
ARTICLES
Published on Web 08/06/2005

Substituent Effects on Redox Potentials and Optical Gap Energies of Molecule-like $Au_{38}(SPhX)_{24}$ Nanoparticles

Rui Guo and Royce W. Murray*

Contribution from the Kenan Laboratories of Chemistry, University of North Carolina, Chapel Hill, North Carolina 27599-3290

Received May 12, 2005; E-mail: rwm@email.unc.edu

Abstract: A molecule-like substituent effect on redox formal potentials in the nanoparticle series $Au_{38}(SPhX)_{24}$ has been discovered. Electron-withdrawing "X" substituents energetically favor reduction and disfavor oxidation, and give formal potentials that correlate with Hammett substituent constants. The ligand monolayer of the nanoparticles is shown, thereby, to play a strong role in determining electronic energies of the nanoparticle core and is more than simply a protecting or capping layer. The substituent effect does not, however, detectably change the HOMO−LUMO gap energy, being identical for the HOMO and LUMO levels and presumably inductive in nature.

Introduction

Unsupported Au nanoparticles with dimensions of a few nanometers and protected by a monolayer of thiolated ligands (MPCs) display interesting properties, such as single-electron charging and molecule-like HOMO−LUMO energy gaps, and offer uses in optical and chemical sensing.[1,2] $Au_{38}(SC2Ph)_{24}$ (SC2Ph = phenylethylthiolate) is an example[3] of a molecule-like nanoparticle, exhibiting a ca. 1.33 eV HOMO−LUMO (highest, lowest occupied molecular orbitals) energy gap, as assessed[4] from redox potential and optical absorbance band-edge measurements. Replacing the original protective ligands of such nanoparticles with new ligands is an important way to introduce new chemical functionalities for various purposes.[2,5,6] This paper reports that, in the case of Au_{38} nanoparticles, changes in the ligand monolayer can *also* provoke substantial change in energies for removing or adding electrons to the core; that is, the monolayer of "monolayer-protected clusters" (MPCs)[2] is more than merely a protective capping shell or source of reactive functionality.

In a recent study[7] of the kinetics of ligand exchanges on $Au_{38}(SC2Ph)_{24}$ MPCs, we found that the original ligands could be exhaustively replaced by *p*-substituted thiophenolate ligands (~100% by ^{1}H NMR), without apparent change in the Au_{38} core. This enabled the preparation of a new series of nanoparticles, $Au_{38}(SPhX)_{24}$ (where X = NO_2, Br, H, CH_3, OCH_3), and allowed subsequent examination of how the substituent "X" affects the core electronic energies, notably the HOMO and LUMO energies and HOMO−LUMO energy gaps of $Au_{38}(SPhX)_{24}$. Substituent effects on reversible redox potentials of small molecules are well-known, as are linear free-energy correlations with Hammett σ constants.[8] Structural effects on redox potentials of polyoxometalate nanoparticles are also known.[9] To our knowledge, there has been, however, no previous observation of substituent effects on redox properties of metal nanoparticles.

Experimental Section

Chemicals. 4-Nitrothiophenol (ACROS, 95%), *p*-toluenethiol (ACROS, 98%), 4-methoxybenzenethiol (ACROS, 98%), phenylethylthiol (PhC2SH, Aldrich, 98%), 4-bromothiophenol (Aldrich, 95%), 4-mercaptophenol (Aldrich, 90%), tetra-*n*-octylammonium bromide (Oct_4NBr, Fluka, 98%), tetrabutylammonium perchlorate (Bu_4NClO_4, Fluka, ≥ 99%), sodium borohydride (Aldrich, 99%), toluene (Fisher), methylene chloride (Fisher), and d_2-methylene chloride (Cambridge Isotope Laboratories, Inc.) were all used as received. Water was purified with a Barnstead NANOpure system.

Synthesis of $Au_{38}(SPhX)_{24}$ Nanoparticles by Ligand Exchange Reactions of Thiophenols HSPhX with $Au_{38}(SC2Ph)_{24}$: Typically, 6 mg of $Au_{38}(SC2Ph)_{24}$ MPCs[7] dissolved in 2 mL of CH_2Cl_2 (not degassed) was reacted with a 4−8 molar excess (molar ratio of HSPhX/PhC2S−) of in-coming thiol HSPhX (X = NO_2, Br, H, CH_3, OCH_3) for periods from overnight to 2 days (depending on the X group;

(1) (a) Storhoff, J. J.; Mirkin, C. A. *Chem. Rev.* **1999**, *99*, 1849. (b) Nam, J. M.; Thaxton, C. S.; Mirkin, C. A. *Science* **2003**, *301*, 1884. (c) Zanchet, D. M.; Micheel, C. M.; Parak, W. J.; Gerison, D.; Alivisatos, A. P. *Nano Lett.* **2001**, *1*, 32. (d) Chen, S.; Ingram, R. S.; Hostetler, M. J.; Pietron, J. J.; Murray, R. W.; Schaaff, T. G.; Khoury, J. T.; Alvarez, M. M.; Whetten, R. L. *Science* **1998**, *280*, 2098.
(2) Templeton, A. C.; Wuelfing, W. P.; Murray, R. W. *Acc. Chem. Res.* **2000**, *33*, 27.
(3) Donkers, R. L.; Lee, D.; Murray, R. W. *Langmuir* **2004**, *20*, 1945.
(4) Lee, D.; Donkers, R. L.; Wang, G.; Harper, A. S.; Murray, R. W. *J. Am. Chem. Soc.* **2004**, *126*, 6193.
(5) (a) Woehrle, G. H.; Warner, M. G.; Hutchison, J. E. *J. Phys. Chem. B* **2002**, *106*, 9979. (b) Woehrle, G. H.; Brown, L. O.; Hutchison, J. E. *J. Am. Chem. Soc.* **2005**, *127*, 2172−2183.
(6) Yang, Y.; Chen, S. *Nano Lett.* **2003**, *3*, 75.
(7) Guo, R.; Song, Y.; Wang, G.; Murray, R. W. *J. Am. Chem. Soc.* **2005**, *127*, 2752−2757.
(8) (a) Zuman, P. *Substituent Effects in Organic Polarography*; Plenum: New York, 1967; Chapter 1, Tables III-1,4. (b) Lin, C.; Fang, M.; Cheng, S. *J. Electroanal. Chem.* **2002**, *531*, 155−162. (c) Graff, J. N.; McElhaney, A. E.; Basu, P.; Gruhn, N. E.; Chang, C.; Enemark, J. H. *Inorg. Chem.* **2002**, *41*, 2642−2647. (d) Batterjee, S. M.; Marzouk, M. I.; Aazab, M. E.; EI-hashash, M. A. *Appl. Organomet. Chem.* **2003**, *17*, 291−297. (e) Johnston, R. F.; Borjas, R. E.; Furilla, J. L. *Electrochim. Acta* **1995**, *40*, 473−477. (f) Hansch, C.; Leo, A.; Taft, R. W. *Chem. Rev.* **1991**, *91*, 165−195.
(9) Keita, B.; Mbomekalle, I.-M.; Nadjo, L.; Haut, C. *Electrochem. Commun.* **2004**, *6*, 978−983.

10.1021/ja053119m CCC: $30.25

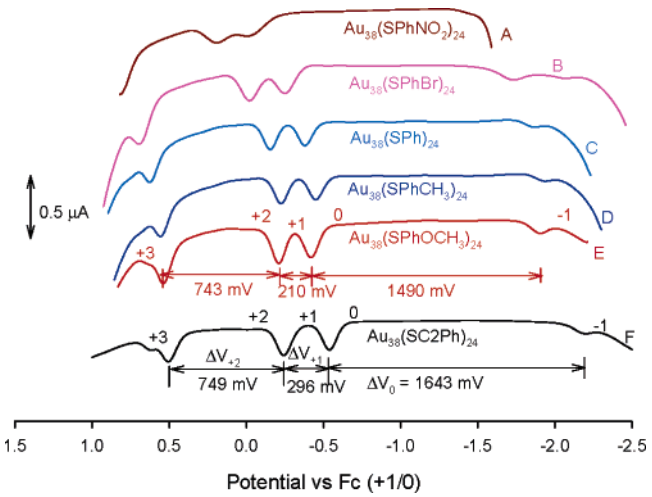

Figure 1. Osteryoung square wave voltammograms (positive-going scan only) of (A) $Au_{38}(SPhNO_2)_{24}$, (B) $Au_{38}(SPhBr)_{24}$, (C) $Au_{38}(SPh)_{24}$, (D) $Au_{38}(SPhCH_3)_{24}$, (E) $Au_{38}(SPhOCH_3)_{24}$, and (F) $Au_{38}(SC2Ph)_{24}$ at 11 °C in 0.1 M Bu_4NClO_4/CH_2Cl_2. The core charge states and spacing between peaks are labeled. The potential scale was calibrated with ferrocene as internal standard (voltammetry not shown).

$HSPhNO_2$ takes less time to reach complete exchange, $HSPhOCH_3$ takes longer). After the reaction, the solvent is evaporated and the product washed copiously with MeOH to remove excess thiol. ^{1}H NMR shows no signal from residual bound PhC2S− ligand, indicating close to 100% ligand exchange.

Measurements. Osteryoung square wave voltammetry (OSWV) was performed at 11 °C in 0.1 M Bu_4NClO_4/CH_2Cl_2 nanoparticle solutions using a Bioanalytical Systems (BAS) Model 100B. (Cyclic voltammograms (not shown) are also routinely taken as a quality check.) The 1.6 mm diameter Pt working electrode was polished, rinsed, and sonicated in NANOpure water, rinsed with absolute ethanol and acetone, and cleaned by potential-cycling in 0.5 M H_2SO_4 for 15 min. A Pt coil counter electrode and a Ag wire quasi-reference electrode were used. Sublimed ferrocene was added as an internal reference.

^{1}H NMR spectra of $Au_{38}(SPhX)_{24}$ and $Au_{38}(SC2Ph)_{24}$ in d_2-methylene chloride were collected with a Bruker AC400 spectrometer. UV−vis spectra of $Au_{38}(SPhX)_{24}$ and $Au_{38}(SC2Ph)_{24}$ in methylene chloride were taken using a Shimadzu UV-1601 UV−visible spectrophotometer.

Results and Discussion

The voltammetry of the new series of nanoparticles $Au_{38}(SPhX)_{24}$ follows a pattern of electron transfers similar[4] to that of the parent, $Au_{38}(SC2Ph)_{24}$, as shown in the square wave voltammetric results of Figure 1. The current peaks for $Au_{38}^{1+/0}$ and $Au_{38}^{2+/1+}$ lie at the formal potentials of those reactions and represent the successive removal of single electrons from the HOMO level. The peak for $Au^{0/-1}$ represents the first reduction step (LUMO energy). These potentials include charging energies.[10] Notably, the peaks shift to more positive potentials—relative to ferrocene$^{0/1+}$ as internal standard—by as much as 450 mV, as X is changed from electron-donating (OCH_3) to electron-withdrawing (NO_2). At the same time, the electrochemical gap, ΔV_0, between the first oxidation peak and the first reduction peak (ca. 1490 ± 10 mV) and ΔV_{+1} between the first and second oxidation peaks (ca. 220 ± 10 mV) are nearly constant within the $Au_{38}(SPhX)_{24}$ nanoparticle series (Table 1).

The observed shifts of the Au_{38} HOMO and LUMO energies with X are consistent with the classical expectation[8] that

Table 1. Osteryoung Square Wave Voltammetry[a] and Optical[b] Absorbance Band-Edge Results for Au_{38} Nanoparticles

	peak spacing[c]				
Au_{38} NPs	ΔV_{+2} (V)	ΔV_{+1} (V)	ΔV_0[d] (V)	$\Delta V_0 - \Delta V_{+1}$[e] (V)	optical band-edge (eV)
$Au_{38}(SPhNO_2)_{24}$	N/A	0.21_8	N/A	N/A	1.30
$Au_{38}(SPhBr)_{24}$	0.71_3	0.22_6	1.50	1.27	1.30
$Au_{38}(SPh)_{24}$	0.75_7	0.21_0	1.49_4	1.28	1.29
$Au_{38}(SPhCH_3)_{24}$	0.76_1	0.22_6	1.48_5	1.26	1.30
$Au_{38}(SPhOCH_3)_{24}$	0.74_3	0.21_0	1.49	1.28	1.30
$Au_{38}(SC2Ph)_{24}$	0.74_9	0.29_6	1.64_3	1.34_7	1.34[f]

[a] Voltammetry acquired at 11 °C in 0.1 M Bu_4NClO_4/CH_2Cl_2. Formal potentials in Figure 2 and peak spacings in this table are averages of peak potentials in positive- and negative-going potential scans to cancel out iR_{UNC} distortion. See Supporting Information for the complete data set. [b] In CH_2Cl_2 solutions. [c] See Figure 1 for definitions of ΔV parameters. Estimated uncertainties in ΔV and band-edges are 0.01−0.02 V. [d] Electrochemical gap. [e] Corrected echem gap. [f] Agrees with previous (ref 4) data (1.33 eV), within experimental uncertainty.

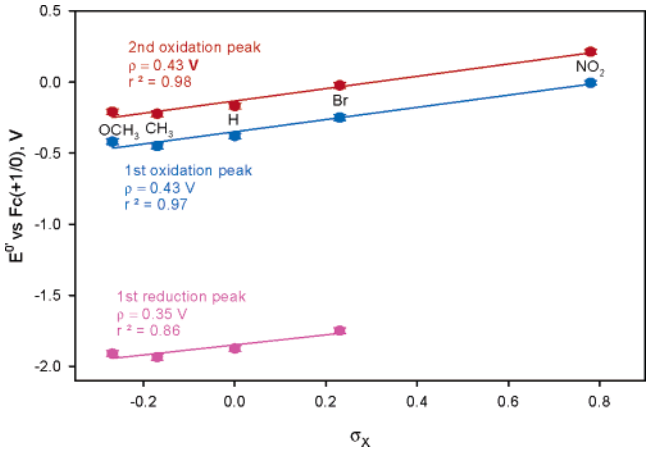

Figure 2. Plot of formal potentials of $Au_{38}(SPhX)_{24}$ couples versus standard substituent σ_X constants (ref 8). (Square wave voltammetry potentials are "half-wave potentials" and differ from true formal potentials $E^{o\prime}$ by log-(ratio of diffusion coefficients of oxidized and reduced forms.) This ratio is not expected to vary significantly with X.)

electron-withdrawing substituents drive the formal potential for oxidation of a molecular electron donor to more positive values. Hammett constants offer one route for analysis of electron inductive effects of molecular substituents (another is outlined below). Figure 2 presents Hammett substituent plots of the formal potentials ($E^{o\prime}$; see Table S-1) of the two oxidation peaks and the one reduction peak of the MPCs $Au_{38}(SPhX)_{24}$. All three plots are reasonably linear, with similar slopes (0.43 V for the oxidations and 0.35 V for the reduction). While these slopes are similar to the 0.1−0.5 V values[8a] common in classical substituent correlations to electrochemical potentials of benzene derivatives, the Au_{38} system is unique in that there are a large number (24) of substituents. Little is known about the spatial distribution of the HOMO and LUMO molecular orbitals that are measured by the voltammetry of the Au_{38} nanoparticles or whether, for example, the electron "hole" in Au_{38}^{1+} is delocalized over the entire core surface or is localized to certain, degenerate kinds of surface sites and undergoes exchange among them. Theory[11a] by Landman for methylthiolate-coated Au_{38} casts the HOMO orbital as a 3-fold degenerate state, concen-

(10) Franceschetti, A.; Zunger, A. *Phys. Rev. B* **2000**, *62*, 2614.

(11) (a) Häkkinen, H.; Barnett, R. N.; Landman, U. *Phys. Rev. Lett.* **1999**, *82*, 3264. (b) Häberlen, O. D.; Chung, S.-C.; Stener, M.; Rösch, N. *J. Chem. Phys.* **1997**, *106*, 5189.

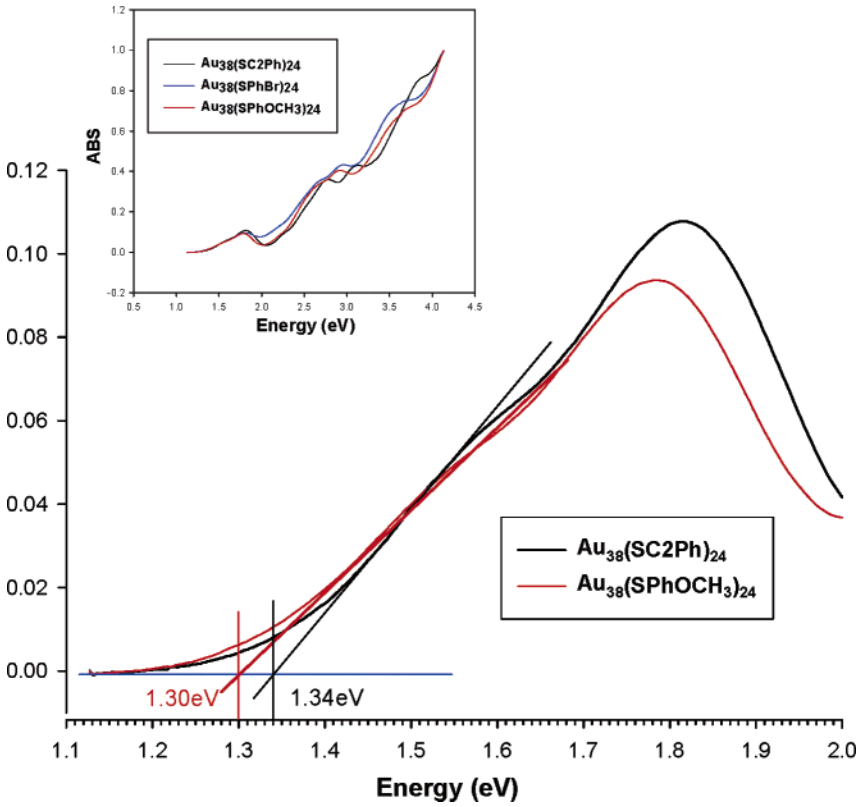

Figure 3. UV−vis spectra of $Au_{38}(SC2Ph)_{24}$, $Au_{38}(SPhBr)_{24}$, and $Au_{38}(SPhOCH_3)_{24}$ nanoparticles in CH_2Cl_2. Inset: spectra at higher energy.

trated around the outermost 24 Au atoms and surrounding 24 sulfur atoms. Other studies suggest a nonuniform chemistry of the Au_{38} core surface, notably variations in Au 4f electron energies,[11b] in ligand exchange kinetics,[7] and luminescence results[12] showing the presence of surface electronic states on their cores. (Extrinsic surface states are well-established[13] as sources of mid-gap luminescence of semiconductor quantum dots.) It seems possible, then, that the HOMO orbital wave function, whose associated redox potentials in Figure 1 are affected by the substituents' properties, is not uniformly distributed over the core surface but has significant amplitude only on a subset of the Au−thiolate bonding sites on the nanoparticle surface (such as the vertices). Whether the orbital is delocalized over those sites is unknown. However, the very presence of substituent effects and Hammett correlation of redox potentials for this small nanoparticle serve to emphasize its molecule-like nature.

The HOMO−LUMO gap energies of the $Au_{38}(SPhX)_{24}$ nanoparticles can be estimated from their electrochemical gap energies (ΔV_0) by correcting for charging energy[10] (a factor associated with solvation/ion association of the electron donor and acceptor states). For $Au_{38}(SC2Ph)_{24}$, we have estimated[4,14] the charging energy from the potential spacing between the first and second oxidation steps ($\Delta V_{+1} = 0.30$ V), giving a corrected gap energy (Table 1) that was in accord with the 1.34 optical band-edge result. Similarly, correcting ΔV_0 for the $Au_{38}(SPhX)_{24}$ nanoparticles (Table 1, "corrected echem gap") gives a (smaller) HOMO−LUMO gap energy of 1.27 ± 0.01 eV that is *unresponsive* to the substituent X; that is, the X substituent must exert a nearly identical electronic effect on both HOMO and LUMO energies. That the estimated $Au_{38}(SPhX)_{24}$ HOMO−LUMO gaps are smaller than that of $Au_{38}(SC2Ph)_{24}$ is consistent with the similar (to $Au_{38}(SC2Ph)_{24}$) 1.33 eV absorbance band-edge energy result[15] for the related hexanethiolate-protected nanoparticle $Au_{38}(SC6)_{24}$. While the effects of X substituents in the $Au_{38}(SPhX)_{24}$ series are presumably largely inductive, the estimated electrochemical (and optical) HOMO−LUMO gap differences between $Au_{38}(SC2Ph)_{24}$ and $Au_{38}(SPhX)_{24}$ MPCs suggest a possible minor role of resonance stabilization (present for $Au_{38}(SPhX)_{24}$ but not $Au_{38}(SC2Ph)_{24}$) of core electronic energies. Resonance interactions of ligands with nanoparticles are an unexplored topic, and study of aromatic thiolated ligands has been initiated.

Optical absorbance band edges are shown in Figure 3 for $Au_{38}(SC2Ph)_{24}$ and $Au_{38}(SPhOCH_3)_{24}$ MPCs. Both spectra show the absorbance shoulder just above the edge associated[4] with HOMO level occupancy. While the steplike higher energy absorbance features of $Au_{38}(SPhX)_{24}$ do vary modestly with X (Figure 3 inset), the optical band-edge energies in the

(12) Wang, G.; Huang, T.; Murray, R. W.; Menard, L.; Nuzzo, R. G. *J. Am. Chem. Soc.* **2005**, *127*, 812.
(13) (a) Shim, M.; Shilov, S. V.; Braiman, M. S.; Guyot-Sionnest, P. *J. Phys. Chem. B* **2000**, *104*, 1494−1496. (b) Fu, H.; Zunger, A. *Phys. Rev. B* **1997**, *56*, 1496−1508. (c) Poles, E.; Selmarten, D. C.; Micic, O. I.; Nozik, A. *J. Appl. Phys. Lett.* **1999**, *75*, 971−973.
(14) The electrochemical gap (ΔV_0) contains charging or addition energy terms (ref 10) that are estimated from the separation between the $Au_{38}^{+2/1+}$ and $Au_{38}^{+1/0}$ formal potentials. That separation (ΔV_{+1}) is roughly represented by a concentric sphere capacitor model, $\Delta V_{+1} = e/C_{MPC} = ed/4\pi\epsilon\epsilon_0 r\,(r + d)$, where e is electron charge, ϵ_0 the permittivity of free space, ϵ the static dielectric constant of the monolayer medium around the metal core, r the is radius of the gold core, and d the thickness of the monolayer medium. The ligand-specific parameters are ϵ and d. The model is approximate since it ignores solvation effects. The *effective* values of ϵ calculated from the model are 5.2 (SC2Ph), 6.5 ($SPhNO_2$), 6.2 (SPhBr), 6.3 (SPhH), 6.3 ($SPhCH_3$), and 7.2 ($SPhOCH_3$), based on d = 7.9, 6.5, 6.4, 5.7, 6.5, and 7.5 Å.
(15) Jimenez, V. L.; Georganopoulou, D. G.; White, R. J.; Harper, A. S.; Mills, A. J.; Lee, D.; Murray, R. W. *Langmuir* **2004**, *20*, 6864.

$Au_{38}(SPhX)_{24}$ series are again unresponsive to X (Table 1) and, while slightly larger than the electrochemical gap estimates, still show a smaller HOMO−LUMO gap relative to $Au_{38}(SC2Ph)_{24}$.

Figure 2 is not a singular analysis of the substituents' effects on redox potentials; an alternative one can be fashioned. Variations in (inductive) Hammett substituent constants are simply indirect representations of substituents' effects on the molecular dipole moments of the thiolated ligands. The collective (and oriented, with respect to the nanoparticle core surface) dipole of the 24 $-NO_2$ substituents in $Au_{38}(SPhNO_2)_{24}$ would bias the core charge positively, effectively causing an increase in the core work function, corresponding changes in nanoparticle ionization potential and electron affinity, and thereby in redox potentials. One can estimate[16] that the 0.45 V shift in the $Au_{38}^{1+/0}$ redox potential can be accounted for by a not-unreasonable difference of ∼1.2 D between the dipole moments of $-SPhCH_3$ and $-SPhNO_2$ ligands. This electrostatic analysis of the redox behavior of $Au_{38}(SPhX)_{24}$ nanoparticles ignores, of course, their molecular character. One is reminded of an analogous "molecular double layer capacitance" representation of electrostatic effects on the relative potentials of serial electron transfers by Weaver.[17]

It is also noteworthy that the previously reported[7,18] rate constants of ligand exchanges in which −SC2Ph ligands are replaced by −SPhX ligands also display a substituent effect, and Hammett correlation, in which $X = NO_2$, leads to the fastest exchange rates (*in either direction* of exchange[7]) and $X = CH_3$ is the slowest. Effects of a substituent on a buildup of charge at the Au−S interface in the rate-determining step of a ligand exchange is obviously consonant with a substituent effect on the energy of loss or gain of electronic charge at that interface.

In summary, this paper describes a molecule-like substituent effect on the redox formal potentials of the nanoparticle series $Au_{38}(SPhX)_{24}$, in which electron-withdrawing substituents energetically favor reduction and disfavor oxidation. The ligand monolayer of the nanoparticles is shown, thereby, to play a strong role in determining the electronic energies in the nanoparticle core. The substituent effect does not, however, produce a change in the HOMO−LUMO gap energy, being identical for the HOMO and LUMO levels, which is consistent with a mainly inductive effect of the ligand.

Acknowledgment. This research was supported in part by grants from the National Science Foundation and the Office of Naval Research. The authors thank Dr. Robert L. Donkers and Prof. Flavio Moran, University of Padova, Italy, for helpful discussions and for sharing their unpublished observations of nanoparticle ligand effects based on a different thiolate ligand. Lanyuan Lu is thanked for help with calculating *r* values.

Supporting Information Available: TEM images of $Au_{38}(SPhOCH_3)_{24}$ and $Au_{38}(SC2Ph)_{24}$, NMR spectra, UV−vis spectra, and formal potentials of $Au_{38}(SPhX)_{24}$ and $Au_{38}(SC2Ph)_{24}$. This material is available free of charge via the Internet at http://pubs.acs.org.

JA053119M

(16) (a) This estimate, suggested by a reviewer, draws on studies[16b] of substituent effects in self-assembled monolayers and the approximate relation $\Delta V \sim N(\mu_{CH3} - \mu_{NO2})/\epsilon\epsilon_0$, where ΔV is redox potential of $X = CH_3$ versus $X = NO_2$, N the area density of the thiolate ligand, μ the ligand dipole moment for indicated substituent, ϵ the static dielectric constant of the ligand shell, and ϵ_o the free space permittivity. ϵ is taken as ∼6.5 for the two ligands from application of a concentric sphere capacitor model[14] to the value of ΔV_{+1}. (b) Campbell, I. H.; Kress, J. D.; Martin, R. L.; Smith, D. L.; Barashkov, N. N.; Ferraris, J. P. *Appl. Phys. Lett.* **1997**, *71*, 3528−3530.

(17) Weaver, M. J.; Gao, X. *J. Phys. Chem.* **1993**, *97*, 332−338.

(18) Donkers, R. L.; Song Y.; Murray, R. W. *Langmuir* **2004**, *20*, 4703−4707.